Published in final edited form as:
Cell. 2013 April 11; 153(2): 348–361. doi:10.1016/j.cell.2013.02.054.

The adapter MAVS promotes NLRP3 mitochondrial localization and inflammasome activation

Naeha Subramanian[1], **Kannan Natarajan**[2], **Menna R. Clatworthy**[1,3], **Ze Wang**[1], and **Ronald N. Germain**[1]

[1]Lymphocyte Biology Section, Laboratory of Systems Biology, National Institute of Allergy and Infectious Diseases, National Institutes of Health, Bethesda, MD, 20892-1892, USA

[2]Molecular Biology Section, Laboratory of Immunology, National Institute of Allergy and Infectious Diseases, National Institutes of Health, Bethesda, MD, 20892-1892, USA

[3]Cambridge Institute for Medical Research, University of Cambridge School of Clinical Medicine, Addenbrooke's Hospital, Cambridge, CB2 0XY, UK

Summary

NLRP3 is a key component of the macromolecular signaling complex called the inflammasome that promotes caspase 1-dependent production of IL-1β. The adapter ASC is necessary for NLRP3-dependent inflammasome function, but it is not known if ASC is a sufficient partner, and whether inflammasome formation occurs in the cytosol or in association with mitochondria is controversial. Here we show that the mitochondria-associated adapter molecule, MAVS, is required for optimal NLRP3 inflammasome activity. MAVS mediates recruitment of NLRP3 to mitochondria, promoting production of IL-1β and the pathophysiologic activity of the NLRP3 inflammasome *in vivo*. Our data support a more complex model of NLRP3 inflammasome activation than previously appreciated, with at least two adapters required for maximal function. Since MAVS is a mitochondria-associated molecule previously considered to be uniquely involved in type 1 interferon production, these findings also reveal unexpected polygamous involvement of PYD/CARD domain-containing adapters in innate immune signaling events.

Introduction

The vertebrate immune system uses a variety of sensors to detect pathogens or tissue damage and mount an inflammatory response for host defense or wound healing. Nod-like receptors (NLRs) are a family of cytosolic proteins containing several prototypic domains, including C-terminal leucine-rich repeats (LRRs), a central nucleotide binding or oligomerization domain (NBD, NOD or NACHT), and N-terminal pyrin domain (PYD) that detect ligands of microbial or endogenous origin and stimulate innate immune activities (Davis et al., 2011). Among NLRs, NLRP3 is perhaps the best studied. NLRP3 forms a macromolecular signaling complex called the inflammasome upon activation by a variety of signals, including infection and metabolic dysregulation, but how these chemically and structurally diverse entities elicit a response from a single sensor molecule is unclear (Gross

Contact Information: Ronald N. Germain, M.D., Ph.D., Office Ph: 301-496-1904, Cell: 301-273-5537, FAX: 301-480-1660, rgermain@nih.gov. Naeha Subramanian, Ph.D., Office Ph: 301-496-0873, FAX: 301-480-1660, subramaniann@niaid.nih.gov.

et al., 2011). One proposed common feature of NLRP3 activators is induction of reactive oxygen species (ROS) (Cruz et al., 2007). The induced ROS is presumed to lead to the generation of a potential ligand of NLRP3 or to modify NLRP3 or associated proteins directly (Zhou et al., 2010). Another reported pathway involves disruption of lysosomes by crystals such as those formed by uric acid or cholesterol, causing release of active cathepsin B that presumably acts as an upstream activator of NLRP3 (Hornung et al., 2008).

Upon activation, NLRP3 oligomerizes with the adapter protein ASC and pro-caspase-1 (Agostini et al., 2004). This results in auto-catalytic cleavage and activation of caspase- 1, which in turn processes pro-forms of IL-1β or IL-18 to produce active cytokine (Cerretti et al., 1992). NLRP3 and ASC are cytosolic proteins, and the assembly of the inflammasome is believed to occur in that cellular compartment. However, organellar recruitment is well recognized for plasma membrane-associated or endosomal TLRs (Blasius and Beutler, 2010) and for the RIG-like helicases (RIG-I and MDA-5) that engage the mitochondrial outer membrane protein MAVS (Mitochondrial Anti-Viral Signaling protein) in pathways leading to the production of type 1 interferon (IFN) (Kawai et al., 2005; Meylan et al., 2005; Seth et al., 2005). A recent report suggests a possible role for mitochondrial recruitment of NLRP3 in inflammasome function (Zhou et al., 2011), but this remains controversial. Some studies implicate mitochondria as the cellular source of ROS and oxidized DNA required for NLRP3 activation (Nakahira et al., 2011; Shimada et al., 2012; Zhou et al., 2011); others indicate that ROS production is required for priming and transcriptional induction of NLRP3 expression, but not for NLRP3 activation (Bauernfeind et al., 2011). If interaction with mitochondria is important for NLRP3 function, how recruitment from the cytosol would be mediated is unclear. CARD and PYD containing proteins can interact with other proteins though homotypic or heterotypic domain-domain interactions (Wagner et al., 2009), but apart from ASC, an adapter known to be crucial for NLRP3 function, data on novel interacting partners in NLRP3 inflammasome assembly or function are just emerging. One additional component participating in NLRP3 inflammasome activity is guanylate binding protein 5 (GBP5) (Shenoy et al., 2012), but there is no evidence this new participant plays any role in connecting the inflammasome to mitochondria.

Although these aspects of the basic biology of the NLRP3 inflammasome remain unresolved, there is little doubt about the role of this signaling system in human disease. Gain of function mutations in NLRP3 are responsible for severe human auto-inflammatory syndromes, and neutralization of the excess active IL-1β rapidly ameliorates symptoms and the pathological effects of the overactive inflammatory process (Goldbach-Mansky and Kastner, 2009). In addition, the NLRP3 inflammasome has been implicated in the inflammatory response to dying cells in the absence of infection (Rock et al., 2010). Such responses are believed to contribute to tissue damage and disease severity, for example, in acute kidney injury (Berry and Clatworthy, 2012).

To clarify the mechanistic aspects of NLRP3 activation, including possible organellar recruitment, we conducted an informatics-based structure-function analysis, which suggested possible mitochondrial localization. Here we demonstrate that NLRP3 associates with mitochondria following activation, which promotes optimal activity of the NLRP3 inflammasome in generating bioactive IL-1β in response to non-crystalline activators. Surprisingly, this recruitment and effect on cytokine generation required the mitochondria-associated adapter protein MAVS, whose interaction with NLRP3 depended on an N-terminal sequence in the latter molecule. MAVS deficiency, like ASC deficiency, protected mice from inflammasome-dependent renal dysfunction and neutrophil influx *in vivo* during sterile inflammation in acute tubular necrosis. Our data thus provide a more comprehensive model of NLRP3 inflammasome activation with two adapters, MAVS and ASC, involved in optimal function through a putatively sequential amplification process involving

mitochondrial membrane recruitment and then effector function. They also reveal an unexpected and novel role for MAVS as a mediator of inflammasome activation beyond its well-defined role in anti-viral immunity and further support a role for mitochondria as platforms integrating multiple innate signaling pathways.

Results

Mitochondrial localization of NLRP3 and ASC

Bioinformatic analysis of localization of NLRP3 using PSORT (Gavel and von Heijne, 1990; Nakai and Kanehisa, 1992) assigned the highest certainty score to mitochondria (Table S1). To investigate if NLRP3 has a propensity to localize to mitochondria, we expressed NLRP3 in HEK-293T cells by transient transfection and visualized NLRP3 and mitochondria. NLRP3 almost completely co-localized with mitochondria under these conditions in which NLRP3 is expressed at supra-physiologic levels in the absence of known activating stimuli (Figures S1A and S1B). In contrast, NLRP2 and NLRP4 did not show such co-localization, indicating that mitochondrial localization was not a general feature of NLR overexpression (Figures S1A and S1B).

HEK-293T cells lack the adapter ASC (Figure S1C), indicating that NLRP3 association with mitochondria does not require ASC. However, since ASC has an indispensible role in NLRP3 inflammasome activity (Agostini et al., 2004), we examined if ASC influences NLRP3 mitochondrial localization. NLRP3 was overexpressed in HEK-293T cells stably expressing cytosolic ASC as a YFP fusion protein (HEK-293-ASC-YFP cells) (Hornung et al., 2009). Over-expression of NLRP3 in these cells led to formation of large cytosolic aggregates (‘speckles’), which include ASC-YFP. NLRP3 localized to mitochondria (Figures S1D and S1E) and ASC formed a speckle that co-localized with NLRP3 and mitochondria (Figures S1D, S1F, S1G and Figure S1I). Such mitochondrial association and speckle formation was not observed for cells over-expressing NLRP4 or NOD1 (Figures S1D–S1I).

We were concerned that this localization of NLRP3 might not reflect the behavior of the molecule in cells with more physiological expression following addition of activating ligands and therefore established a stable expression system in which NLRP3 mRNA was transcribed in pyroptosis-resistant HEK-293T cells under the control of an inducible tetracycline promoter (Shin et al., 2006). HEK-293T cells lack P2X receptors and have low phagocytic ability (Gu et al., 2010), making them relatively resistant to some NLRP3-activating stimuli like ATP and crystalline substances such as MSU and alum. Therefore, nigericin, an ionophore that catalyzes an electroneutral potassium/proton exchange across lipid bilayers to induce NLRP3 activation, was used as the stimulus.

Expression of NLRP3 was induced in stable transfectants by doxycycline (DOX) and the cells analyzed by confocal microscopy. When expressed at more physiological levels, NLRP3 was cytosolic in the resting state but localized to mitochondria upon activation with nigericin (Figures 1A and 1B). Similar results were obtained under transient expression conditions in cells showing very low, and therefore closer to physiological, expression levels (Figures 1C and 1D). The fraction of NLRP3 that translocated to mitochondria upon nigericin stimulation was about three to five fold lower than that observed under over-expression conditions (Figures S1B, S1E, 1B and 1D). These results indicate that the mitochondrial localization of NLRP3 observed under over-expression conditions in Figure S1 reflected an activated phenotype, where forced self-association and/or oligomerization of NLRP3 by expression at supra-physiological levels in HEK-293T cells was sufficient to drive NLRP3 to the mitochondria. Consistent with these imaging data, subcellular fractionation studies of wild-type (WT) bone marrow-derived macrophages (BMDMs)

showed that NLRP3 was predominantly cytosolic in untreated, resting BMDMs and localized to the mitochondrial fraction upon activation with nigericin (Figure 1E). Similar results were obtained in ASC KO BMDMs, confirming the ASC-independent nature of activation-induced NLRP3 mitochondrial localization (Figure 1E).

Mapping of the mitochondrial association sequence of NLRP3

To determine whether the PSORT-predicted N-terminal mitochondrial pre-sequence in NLRP3 was involved in recruitment of activated NLRP3 to mitochondria, we conducted a mutagenesis study. When expressed in HEK-293-ASC-YFP cells under transient low expression conditions, a deletion mutant of NLRP3 that lacked 20 amino acids at the N-terminus (NLRP3 Δ 2-21) (Figure 2A) exhibited complete loss of mitochondrial localization and ASC speckle formation under both unstimulated (Figure S2, WT and Δ 2-21 panels) and nigericin-activated conditions (Figure 2B, WT and Δ 2-21 panels). To more precisely map the relevant sequence, we generated a series of N-terminal deletion mutants of NLRP3 (Δ 2-3, Δ 2-5, Δ 2-7, Δ 2-9, Δ 2-11, and Δ 2-21; Figure 2A), and examined their behavior using a transient, low expression system in HEK-293-ASC-YFP cells. The deletion mutants retained their ability to self-associate and were expressed at levels similar to the WT NLRP3 (Figures S3A and S3B). Importantly, the Δ 2-3, Δ 2-5, Δ 2-7, and Δ 2-9 deletions of NLRP3 preserved all the residues implicated in stability of the pyrin domain in the NLRP3 PYD crystal structure (Bae and Park, 2011).

Under unstimulated conditions, WT NLRP3 and its N-terminal deletions were primarily localized to the cytosol (Figure S2), with just a small proportion of the WT and Δ 2-3 NLRP3, and an even lesser proportion of the Δ 2-5 NLRP3 co-localized with mitochondria in the higher expressing cells of the population (Figure S2). These cells with low levels of NLRP3-mitochondria association also showed ASC speckle formation (Figure S2, quantification in Figure 3A), consistent with the notion that ASC aggregation is an autocatalytic process that proceeds rapidly following a speck nucleation event in the presence of NLRP3 (Cheng et al., 2010). None of the other NLRP3 mutants (Δ 2-7, Δ 2-9, Δ 2-11, and Δ 2-21) showed this low level of mitochondrial association and ASC aggregation in the absence of inflammasome activating stimuli (Figure S2).

When stimulated with nigericin, markedly increased levels of WT NLRP3 associated with mitochondria, but the N-terminal deletions progressively lost their ability to associate with mitochondria and to form aggregates with ASC (Figure 2B, quantification in Figures 3B and 3C). The Δ 2-7 deletion mutant, exhibited remarkably diminished mitochondrial association and ASC speckle formation, and the Δ 2-9 and Δ 2-11 deletion mutants showed a complete loss of these properties (Figure 2B, quantification in Figures 3B and 3C). Many cells expressing the Δ 2-5 mutant showed incomplete ASC aggregation and all of the cells expressing the Δ 2-7 mutant showed either incomplete or no ASC speckle formation (Figure 3B). Incompletely developed ASC speckles in these cells appeared as rudimentary, thread-like structures (Figure 2B). Taken together, these results indicated that residues 2-7 (KMASTR) constituted a minimum N-terminal sequence necessary for both NLRP3 mitochondrial association and maximal ASC aggregation (Figure 3D), and that these processes were likely coupled. The disabling mutations reduced mitochondrial association and speckle formation but did not prevent NLRP3 self-association (Figure S3A), suggesting that NLRP3 oligomerization and its recruitment to mitochondria were separable functions, and that some types of NLRP3 self-association (as shown in Figure S3A for the Δ 2-9 and Δ 2-21 mutants) were not adequate to promote ASC condensation.

Consistent with these localization data, endogenous NLRP3-expressing THP-1 cells stably co-expressing the NLRP3 Δ 2-21 mutant under the control of a tetracycline-inducible promoter lost their ability to secrete IL-1β in response to moderate levels of known NLRP3-

activators (Figure 3E), implying a dominant negative activity of this truncated protein. Since the Δ 2-21 mutant retained its ability to self-associate (Figure S3A), it is likely that this mutant exerted its dominant negative function by scavenging the endogenous NLRP3 into defective oligomeric complexes incapable of mitochondria-associated downstream signaling. In agreement with these functional data, subcellular fractionation of stably transduced HEK-293T cells showed markedly diminished levels of the Δ 2-21 NLRP3 mutant in the mitochondrial fraction as compared to the WT NLRP3, following induction with DOX and activation with nigericin (Figure 3F).

Identification of MAVS as critical to NLRP3 recruitment to mitochondria

We next asked whether an interacting mitochondrial partner guides NLRP3 to this location. MAVS is a well-known mitochondrial protein that plays a crucial role in RIG-like receptor (RLR) signaling pathways leading to type I IFN induction and NF-κB activation (Kawai et al., 2005; Meylan et al., 2005; Seth et al., 2005). MAVS plays a role in maintaining intestinal homeostasis and MAVS−/− mice do not upregulate IL-1β in an experimental model of colitis (Li et al., 2011). Other studies suggest that NLRs can engage in heterotypic protein-protein interactions (Bruey et al., 2007; Eitas and Dangl, 2010; Hsu et al., 2008; Wagner et al., 2009). We therefore examined whether MAVS might guide NLRP3 to the mitochondria by silencing MAVS in HEK-293T cells. Treatment of HEK-293T cells with either of two different MAVS siRNAs, but not control siRNAs, markedly reduced NLRP3 association with mitochondria following transient over-expression of NLRP3 (Figures 4A and 4C and Movies S1–S2). We observed a similar dependence on MAVS for nigericin-induced NLRP3 association with mitochondria in a transient low expression system (Figures 4B and 4D). Biochemical studies showed increased association between NLRP3 and MAVS in bone-marrow derived macrophages (BMDM) upon treatment with NLRP3-activating stimuli, but not upon exposure to stimuli that activate other NLR family members, such as NLRC4 (flagellin), NLRP1/NOD2 (MDP), or AIM2 (transfected DNA) (Figure 4E and Figures S4E–S4F). Such NLRP3-MAVS association in macrophages did not correlate with cell death (Figure S4G). Congruent results were obtained in immunoprecipitation and imaging studies in HEK-293T cells (Figures S4A–S4C). In accord with their impaired capacity to show mitochondrial recruitment, N-terminal deletion mutants of NLRP3 also progressively lost their ability to engage MAVS, based on co-immunoprecipitation analysis following cell exposure to nigericin as well as direct binding studies utilizing *in vitro* translated NLRP3 and recombinant, soluble MAVS protein (Figures 4F and 4H and Figure S4D). A significant loss of association with MAVS was observed progressively starting with the Δ 2-7 mutant (Figure 4F), implying that this region of NLRP3 mediated its mitochondrial recruitment activity by promoting direct NLRP3-MAVS interaction. Furthermore, adding the N-terminus of NLRP3 to NLRP4, an NLR that does not show mitochondrial localization, conferred on this molecule the ability to associate with MAVS both in co-immunoprecipitation experiments as well as in direct binding studies using purified proteins (Figures 4G and 4H), showing that the N-terminus of NLRP3 was not only necessary but could be sufficient for promoting direct association with MAVS.

Functional role of MAVS in NLRP3-mediated production of mature IL-1β

NLRP3 inflammasome assembly leads to caspase-1 activation and processing of pro-IL-1β (Agostini et al., 2004). We thus investigated a role for mitochondrial localization via MAVS in NLRP3 inflammasome-mediated IL-1β generation. MAVS was silenced in BMDMs from C57BL/6 mice prior to LPS priming and stimulation with NLRP3, NLRC4, or AIM2 activators and secreted IL-1β measured by ELISA. Treatment with MAVS siRNA but not control siRNA reduced IL-1β secretion in response to NLRP3 activators ATP, nigericin, and poly I:C, but not NLRC4 activator flagellin or AIM2 activator poly dA:dT, in a dose-dependent manner, indicating that MAVS played an amplifying role in NLRP3-dependent

IL-1β secretion (Figures 5A–5F). Congruent results were obtained in macrophages derived from MAVS −/− mice by ELISA (Figures 6A–6F and Figures S5C–S5F) and immunoblotting (Figure 6G and Figures S5A–S5B). MAVS −/− macrophages showed normal priming of NLRP3, pro-IL-1β and pro-caspase-1 expression (Figures 6G–6H and Figures S5A–S5B) and displayed normal mitochondrial/MAMS (mitochondria-associated ER membranes) architecture (Figure S5G). However, these cells showed markedly reduced processing of caspase-1 and secretion of mature IL-1β in response to sub-saturating concentrations of the NLRP3 activators ATP, nigericin, and poly I:C, though not in response to NLRC4 or AIM2 activators (Figures 6A–6B, 6D–6F, 6G and Figures S5C and S5F), indicating that MAVS was required for optimal NLRP3 inflammasome activation in myeloid cells *in vitro*. There was a graded dependence on MAVS for caspase-1 activation and IL-1β secretion depending upon the dose and nature of the NLRP3 activator used, with poly I:C, ATP, and nigericin showing maximal dependence on MAVS (in the order poly I:C > ATP, nigericin; Figures 6A–6B, 6D, 6G and Figure S5C). Caspase-1 and IL-1β processing in response to crystalline substances such as alum, CPPD, and MSU, was, however, largely independent of MAVS (Figures 6C, 6G and Figures S5D–S5E) and MAVS −/− mice were not reproducibly protected from crystal-induced peritonitis (Figure S6D). Thus, although NLRP3 has been shown to localize to the mitochondrial/MAM fraction upon activation with crystalline activators such as MSU (Zhou et al., 2011), other factors besides MAVS may mediate this recruitment.

ASC is crucial for assembly of the NLRP3 inflammasome, which yields a pyroptosome composed of ASC dimers and/or oligomers that localizes to a detergent-insoluble fraction in the cell (Fernandes-Alnemri et al., 2007). Since our imaging and biochemical data in HEK-293T cells suggested that NLRP3 mitochondrial localization and engagement of MAVS was independent of ASC, we hypothesized that NLRP3 association with MAVS might be upstream of its interaction with ASC. Indeed, immunoblotting of the detergent-resistant fraction following activation of BMDMs with sub-saturating concentrations of non-crystalline NLRP3 activators showed reduced ASC oligomerization and localization to the detergent-resistant fraction in macrophages from MAVS−/− mice compared to WT mice (Figure 6G). These data suggested that MAVS was required for highly efficient NLRP3 inflammasome activation resulting in maximal ASC oligomerization/pyroptosome formation and subsequent secretion of mature IL-1β (as depicted in Figure S7).

MAVS has a well-established role in induction of type 1 IFN in response to viral infection. To determine if NLRP3 interaction with MAVS led to type 1 IFN production, we analyzed human monocytes following treatment with LPS-ATP, an exclusive activator of NLRP3 (Mariathasan et al., 2006), or infection with Influenza A strain HKX31, a known activator of the RIG-I-MAVS pathway (Pichlmair et al., 2006). Treatment with LPS-ATP induced IL-1β expression in monocytes, but minimal amounts of IFN-β over what would be expected from TRIF-dependent LPS signaling). In contrast, infection with Influenza A virus HKX31 induced robust IFN-β expression, but negligible IL-1β expression (Figure 5G), suggesting that these pathways might be mutually exclusive under these conditions.

Importance of MAVS in an in vivo model of inflammasome-mediated immunopathology

Finally, we addressed the role of MAVS in inflammasome activation *in vivo* using a model of sterile inflammation, folic acid-induced acute tubular necrosis (ATN). Folic acid-induced acute kidney injury is characterized by necrosis of tubular cells, and IL-1β and IL-18 are key promoters of the inflammatory response to dying cells and subsequent tissue damage during ATN (Furuichi et al., 2006; Haq et al., 1998). NLRP3, ASC, and caspase-1-deficient mice are protected from ATN, establishing a critical role for the NLRP3 inflammasome in this model of sterile damage (Berry and Clatworthy, 2012; Faubel et al., 2004; Iyer et al., 2009). Remarkably, MAVS-deficient mice, like ASC-deficient mice, were protected from weight

loss, renal dysfunction, and renal pathology during ATN (Figures 7A–7C and Figure S6C). This protection was associated with a reduction in interstitial neutrophil infiltration (Figures 7D and 7E) and IL-1β staining in the kidneys of ASC and MAVS-deficient mice compared to WT mice (Figures 7F and 7G). Priming of NLRP3 and pro-IL-1β expression in the kidney during ATN was normal in MAVS −/− and ASC −/− mice (Figures S6A and S6B). Together, these data indicated that MAVS, like ASC, was an important mediator of NLRP3 activation *in vivo* that was required for the sterile inflammatory response in ATN.

Discussion

The existing paradigm for NLR signaling is oligomerization with a single adapter protein that mediates information transfer to a downstream effector. In the case of NLRP3, this involves interaction of its PYD domain with a similar domain on ASC, which through CARD domain interactions promotes conversion of pro-caspase-1 to its enzymatically active form. The latter then cleaves pro-IL-1β to generate the biologically functional cytokine. Here we provide evidence that this paradigm is incomplete. For optimal activity of the NLRP3 inflammasome, two adapters are required. In addition to ASC, MAVS is needed and acts to promote recruitment of NLRP3 to the mitochondria. This recruitment, which depends on a short N-terminal sequence in NLRP3, then promotes ASC ‘speckle’ formation and the downstream biochemical events associated with the activity of the inflammasome (Figure S7). Overall, these findings suggest a much more subtle and complex organization of microbial and tissue damage sensing pathways than has been considered to date. They also generalize the important role already ascribed to intracellular relocalization in the operation of some cytosolic sensors such as RIG-I, an event whose importance in NLRP3 inflammasome function has been controversial.

Although MAVS is well recognized for promoting expression of IFN-β downstream of RIG-I and MDA-5 detection of viral RNA (Kawai et al., 2005), MAVS interaction with NLRP3 in response to ATP contributed specifically to inflammasome-dependent generation of IL-1β but not to induction of IFN-β (Figure 5G). How might this occur? A recent study suggests that virus infection induces the formation of detergent-resistant, fibril-like, high molecular weight aggregates of the MAVS protein and that these aggregates are potent activators of IRF3 (Hou et al., 2011). It remains to be examined whether NLRP3 activators induce formation of such MAVS aggregates. However, given our observation of negligible induction of IL-1β by Influenza A virus (Figure 5G), one possibility is that formation of MAVS fibrils might be an exclusive characteristic of RIG-I activation and that the lack or inhibition of such MAVS aggregation by NLRP3 activators might permit this adapter to promote ASC-dependent IL-1β generation without activating the IRF3-interferon pathway. These observations suggest a modified model for adapter function, in which the biological outcome of signaling is determined by the interplay of the adapter (i.e., MAVS) with the upstream sensor (i.e., RIG-I versus NLRP3) rather than by the properties of the adapter *per se*.

In the case of activators such as poly I:C that are believed to have a dual role in both MDA-5-dependent type 1 IFN and NLRP3-dependent IL-1β signaling (Rajan et al., 2010), the specificity of MAVS signaling could be dictated by the stimulus dose or duration and cytosolic sensor expression. For instance, in unprimed macrophages, poly I:C induces robust MDA-5 and MAVS-dependent type 1 IFN but not NLRP3-dependent IL-1β secretion. However, following transcriptional induction of NLRP3 and pro-IL-1β expression by NF-κB activators like LPS, macrophages show NLRP3-dependent and MDA-5 independent IL-1β secretion in response to poly I:C (Rajan et al., 2010). Thus, the expression levels of the cytosolic sensors might dictate which sensor (NLRP3 or MDA-5) engages MAVS and the subsequent signaling pathway that is triggered.

How do NLRP3 and MAVS interact? Our imaging, biochemical, and direct binding data (Figures 2B, 3C, 4F, 4H and Figure S4D) indicate that residues 2-7 at the N-terminal of NLRP3 constitute a minimum sequence that mediates NLRP3-MAVS interaction and localization of activated NLRP3 to mitochondria. Indeed, adding the N-terminus (2-11) of NLRP3 to NLRP4, an NLR that does not show mitochondrial localization, confers on it the ability to associate with MAVS (Figures 4G and 4H) suggesting that the N-terminus of NLRP3 itself plays a major role in mediating binding to MAVS.

Given the large size of the inflammasome (Stutz et al., 2009), and the capacity of NLR proteins to engage in homotypic and heterotypic protein-protein interactions (Eitas and Dangl, 2010; Wagner et al., 2009), it is possible that in addition to MAVS, there might be other interacting partners, mitochondrial and/or non-mitochondrial, which constitute the fully active NLRP3 inflammasome. In this regard, a recent report shows that a non-NLR protein, GBP5 (guanylate binding protein 5), stimulates selective NLRP3 inflammasome assembly (Shenoy et al., 2012). Moreover, our *in vitro* IL-1β data reveal a varied dependence on MAVS for IL-1β secretion depending upon the nature and dose of the NLRP3 activator, with poly I:C, ATP, and nigericin showing maximal dependence on MAVS, and crystalline substances showing minimal dependence on MAVS for IL-1β secretion (Figures 6A–6D and S5C–S5E), suggesting that other factors besides MAVS may mediate NLRP3 mitochondrial recruitment in response to crystalline activators. Nonetheless, our results in ATN, an *in vivo* model of sterile inflammation, suggest that MAVS is as important as ASC in inducing neutrophil influx and IL-1β production in response to tissue injury and necrosis (Figures 7D–7G). This indicates that at physiologically-relevant levels of stimulation, there is a similar dependence on MAVS and ASC for inflammasome activation.

Taken together, our findings reveal a previously undescribed mechanism by which NLRP3 localization to the mitochondria and inflammasome activation are regulated by the mitochondrial adapter protein MAVS, and identify an N-terminal sequence in NLRP3 that supports its association with MAVS. These data strengthen the view that mitochondria act as platforms facilitating innate immune responses and add to our understanding of the molecular complexity of sensor and adapter interactions that promote effective host defense.

Experimental Procedures

Detailed methods are described in ‘Extended Experimental Procedures’ in the supplement.

Mice

ASC −/− and MAVS +/− mice were kindly provided by Drs. V. Dixit, Genentech and Z. Chen, UT Southwestern, respectively. As heterozygous MAVS +/− mice provided to us were 129/Sv × C57BL/6 hybrids, littermates from the crossing of heterozygous mice were used in individual experiments. All procedures were approved by the NIAID Animal Care and Use Committee (National Institutes of Health, Bethesda, MD).

Constructs and stable cell lines

Generation of NLRP2, NLRP4, NOD1, and NLRP3 constructs, and lentivirally transduced, DOX-inducible HEK-293T and THP-1 cell lines expressing NLRP3 are described in ‘Extended Experimental Procedures’. NLRP3 expression was induced with 1 μg/ml DOX for 12 h. HEK-293-ASC-YFP cells were a kind gift of Dr. E. Latz, University of Bonn, Germany.

Transfections

HEK-293T and HEK-293-ASC-YFP cells were seeded on poly-L-lysine coated 2 chambered coverglass slides (Lab-tek, NUNC) and transfected with siRNA oligos (100 nM) using Lipofectamine 2000 (Invitrogen) or plasmid DNA (1 μg DNA/10^6 cells for 20 h for over-expression or 0.1 μg DNA/10^6 cells for 8 h for transient low expression) using Fugene 6 (Roche).

Immunofluorescence Staining and Confocal microscopy

HEK-293T cells were stained with Mitotracker Red (50 nM, 20 min, 37°C, Molecular Probes, Invitrogen), fix-permeabilized (BD cytofix-cytoperm), and stained with primary antibodies (anti-NLRP3; Nalpy3a/Nalpy3b, Abcam or anti-FLAG M2 antibody, Sigma), and suitable Alexa Fluor-conjugated secondary antibodies (Molecular Probes, Invitrogen). Images were acquired on a Leica SP5 Confocal Imaging System with a z-step size of 0.5 μm to 1 μm and processed with Imaris software.

Cell fractionation

Mitochondria were isolated from cells using a Mitochondria Isolation Kit (Thermo Scientific) or as previously described (Wieckowski et al., 2009), lysed in 2% SDS and boiled with 2X reducing sample buffer for SDS-PAGE.

Inflammasome activation

HEK-293T cells were treated with 15 μM nigericin (Sigma) for 45 minutes prior to imaging. Poly I:C was obtained from Amersham Biosciences. All other inflammasome stimulants were from InvivoGen. PMA-differentiated THP-1 cells and LPS-primed BMDMs or peritoneal macrophages were treated with ATP (1.25 mM, 2.5 mM or 5 mM) or nigericin (3.75 μM, 7.5 μM or 15 μM) for 20 min, MSU or alum crystals (200 μg/ml), poly I:C or poly dA:dT (indicated concentrations) for 6 h and MDP (5 μg/ml), flagellin or CPPD crystals (indicated concentrations) for 2 h. For detection of ASC oligomerization, pellets from whole-cell lysates were cross-linked with disuccinimidyl suberate (DSS; Thermo Scientific) and boiled with 1X sample buffer for immunoblot analysis.

Direct binding assays

MAVS was expressed in Drosophila S2 cells and purified from the medium by Ni-NTA (Qiagen) and size exclusion chromatography. FLAG-tagged WT and mutant NLR proteins were prepared by *in vitro* translation using a reticulocyte lysate system (TNT T7 Quick Coupled Transcription/Translation System, Promega). The synthesized protein was captured on anti-FLAG coated beads, and used in pull down assays with 5 μg of purified MAVS protein.

Immunoprecipitation and Immunoblot Analysis

Proteins in whole cell lysates were immunoprecipitated with primary antibody for 4 h at 4°C followed by anti-mouse or anti-rabbit Dynabeads (Invitrogen) for 1 h at 4°C, eluted with 1X SDS reducing sample buffer, electrophoresed on 4–20% Novex® Tris-Glycine Gels (Invitrogen), transferred to nitrocellulose (Bio-Rad), probed with primary antibody followed by HRP-conjugated secondary antibodies, and developed with SuperSignal Chemiluminescence Substrate (Thermo Scientific). The following primary antibodies were used: NLRP3 (Nalpy3a/Nalpy3b, Abcam; Cryo-2, Enzo life sciences), FLAG M2 (Sigma), HA (Sigma), human Cardif (Enzo life sciences), MAVS (rodent specific, Cell Signaling Technology); IL-1β caspase-1 and ASC (Santacruz Biotech) and mouse IL-1β (R&D Systems).

ELISA

IL-1β in supernatants was measured using a IL-1β ELISA Kit (BD OptEIA; BD Biosciences) following the manufacturer's instructions.

Quantitative RT-PCR

Total RNA was extracted using RNAeasy Mini Kit (Qiagen). Quantitative RT-PCR for IL-1β and IFN-β was performed using FAM-labeled TaqMan MGB probes (Applied Biosystems). mRNA levels were normalized to GAPDH expression.

Folic acid-induced Acute Tubular Necrosis

Folic acid (250 mg/kg, Sigma) or vehicle (150 mM sodium bicarbonate) was administered i.p. Mice were weighed at 0, 12, 24, and 36 hours post-treatment, euthanized by CO_2 asphyxiation at 36 h, and blood samples and kidneys were collected. Sera were evaluated for BUN (blood urea nitrogen). One kidney was processed for hematoxylin-eosin staining and the other for immunofluorescence staining (see 'Extended Experimental Procedures'). Interstitial neutrophil infiltration and IL-1β positive cells were quantitated on 30 μm kidney sections stained with anti-Ly6G (1A8, BD Biosciences) or anti-IL-1β (R&D Systems), together with a PECAM-1 antibody to identify extravascular, interstitial neutrophils. Images were acquired on a 710 confocal microscope (Zeiss) with a z-step size of 2 μm. Raw images were processed and analyzed with Imaris (Bitplane).

Statistical analyses

Two-tailed, unpaired Student's t tests were performed to analyze statistical differences between groups (Prism, GraphPad). p values < 0.05 were considered statistically significant.

Supplementary Material

Refer to Web version on PubMed Central for supplementary material.

Acknowledgments

This work was supported by the Intramural Research Program, NIAID, NIH, and a Wellcome Trust Intermediate Fellowship (WT081020) to M.R.C. We are grateful to Drs. Daniel Kastner, Michael Lenardo, and Iain Fraser for critical reading of the manuscript. We thank the Biological Imaging Section, NIAID, NIH for excellent imaging support, Dr. Vishva Dixit and Dr. Zhijian Chen for kindly providing mouse strains, Dr. Eicke Latz for generously providing HEK-293-ASC-YFP cells, Dr. Iain Fraser for providing lentiviral constructs and Drs. Wolfgang Kastenmuller, Marlene Brandes and Jae Jin Chae for helpful discussions. The authors declare that they have no competing financial interests.

References

Agostini L, Martinon F, Burns K, McDermott MF, Hawkins PN, Tschopp J. NALP3 forms an IL-1beta-processing inflammasome with increased activity in Muckle-Wells autoinflammatory disorder. Immunity. 2004; 20:319–325. [PubMed: 15030775]

Bae JY, Park HH. Crystal structure of NALP3 protein pyrin domain (PYD) and its implications in inflammasome assembly. J Biol Chem. 2011; 286:39528–39536. [PubMed: 21880711]

Bauernfeind F, Bartok E, Rieger A, Franchi L, Nunez G, Hornung V. Cutting edge: reactive oxygen species inhibitors block priming, but not activation, of the NLRP3 inflammasome. J Immunol. 2011; 187:613–617. [PubMed: 21677136]

Berry M, Clatworthy MR. Immunotherapy for acute kidney injury. Immunotherapy. 2012; 4:323–334. [PubMed: 22401637]

Blasius AL, Beutler B. Intracellular toll-like receptors. Immunity. 2010; 32:305–315. [PubMed: 20346772]

Bruey JM, Bruey-Sedano N, Luciano F, Zhai D, Balpai R, Xu C, Kress CL, Bailly-Maitre B, Li X, Osterman A, et al. Bcl-2 and Bcl-XL regulate proinflammatory caspase-1 activation by interaction with NALP1. Cell. 2007; 129:45–56. [PubMed: 17418785]

Cerretti DP, Kozlosky CJ, Mosley B, Nelson N, Van Ness K, Greenstreet TA, March CJ, Kronheim SR, Druck T, Cannizzaro LA, et al. Molecular cloning of the interleukin-1 beta converting enzyme. Science. 1992; 256:97–100. [PubMed: 1373520]

Cheng J, Waite AL, Tkaczyk ER, Ke K, Richards N, Hunt AJ, Gumucio DL. Kinetic properties of ASC protein aggregation in epithelial cells. Journal of cellular physiology. 2010; 222:738–747. [PubMed: 20020448]

Cruz CM, Rinna A, Forman HJ, Ventura AL, Persechini PM, Ojcius DM. ATP activates a reactive oxygen species-dependent oxidative stress response and secretion of proinflammatory cytokines in macrophages. J Biol Chem. 2007; 282:2871–2879. [PubMed: 17132626]

Davis BK, Wen H, Ting JP. The inflammasome NLRs in immunity, inflammation, and associated diseases. Annu Rev Immunol. 2011; 29:707–735. [PubMed: 21219188]

Eitas TK, Dangl JL. NB-LRR proteins: pairs, pieces, perception, partners, and pathways. Current opinion in plant biology. 2010; 13:472–477. [PubMed: 20483655]

Faubel S, Ljubanovic D, Reznikov L, Somerset H, Dinarello CA, Edelstein CL. Caspase-1-deficient mice are protected against cisplatin-induced apoptosis and acute tubular necrosis. Kidney international. 2004; 66:2202–2213. [PubMed: 15569309]

Fernandes-Alnemri T, Wu J, Yu JW, Datta P, Miller B, Jankowski W, Rosenberg S, Zhang J, Alnemri ES. The pyroptosome: a supramolecular assembly of ASC dimers mediating inflammatory cell death via caspase-1 activation. Cell death and differentiation. 2007; 14:1590–1604. [PubMed: 17599095]

Furuichi K, Wada T, Iwata Y, Kokubo S, Hara A, Yamahana J, Sugaya T, Iwakura Y, Matsushima K, Asano M, et al. Interleukin-1-dependent sequential chemokine expression and inflammatory cell infiltration in ischemia-reperfusion injury. Critical care medicine. 2006; 34:2447–2455. [PubMed: 16849996]

Gavel Y, von Heijne G. Cleavage-site motifs in mitochondrial targeting peptides. Protein engineering. 1990; 4:33–37. [PubMed: 2290832]

Goldbach-Mansky R, Kastner DL. Autoinflammation: the prominent role of IL-1 in monogenic autoinflammatory diseases and implications for common illnesses. The Journal of allergy and clinical immunology. 2009; 124:1141–1149. quiz 1150-1141. [PubMed: 20004775]

Gross O, Thomas CJ, Guarda G, Tschopp J. The inflammasome: an integrated view. Immunol Rev. 2011; 243:136–151. [PubMed: 21884173]

Gu BJ, Saunders BM, Jursik C, Wiley JS. The P2X7-nonmuscle myosin membrane complex regulates phagocytosis of nonopsonized particles and bacteria by a pathway attenuated by extracellular ATP. Blood. 2010; 115:1621–1631. [PubMed: 20007545]

Haq M, Norman J, Saba SR, Ramirez G, Rabb H. Role of IL-1 in renal ischemic reperfusion injury. Journal of the American Society of Nephrology: JASN. 1998; 9:614–619. [PubMed: 9555664]

Hornung V, Ablasser A, Charrel-Dennis M, Bauernfeind F, Horvath G, Caffrey DR, Latz E, Fitzgerald KA. AIM2 recognizes cytosolic dsDNA and forms a caspase-1-activating inflammasome with ASC. Nature. 2009; 458:514–518. [PubMed: 19158675]

Hornung V, Bauernfeind F, Halle A, Samstad EO, Kono H, Rock KL, Fitzgerald KA, Latz E. Silica crystals and aluminum salts activate the NALP3 inflammasome through phagosomal destabilization. Nat Immunol. 2008; 9:847–856. [PubMed: 18604214]

Hou F, Sun L, Zheng H, Skaug B, Jiang QX, Chen ZJ. MAVS forms functional prion-like aggregates to activate and propagate antiviral innate immune response. Cell. 2011; 146:448–461. [PubMed: 21782231]

Hsu LC, Ali SR, McGillivray S, Tseng PH, Mariathasan S, Humke EW, Eckmann L, Powell JJ, Nizet V, Dixit VM, et al. A NOD2-NALP1 complex mediates caspase-1-dependent IL-1beta secretion in response to Bacillus anthracis infection and muramyl dipeptide. Proc Natl Acad Sci U S A. 2008; 105:7803–7808. [PubMed: 18511561]

Iyer SS, Pulskens WP, Sadler JJ, Butter LM, Teske GJ, Ulland TK, Eisenbarth SC, Florquin S, Flavell RA, Leemans JC, et al. Necrotic cells trigger a sterile inflammatory response through the Nlrp3 inflammasome. Proc Natl Acad Sci U S A. 2009; 106:20388–20393. [PubMed: 19918053]

Kawai T, Takahashi K, Sato S, Coban C, Kumar H, Kato H, Ishii KJ, Takeuchi O, Akira S. IPS-1, an adaptor triggering RIG-I- and Mda5-mediated type I interferon induction. Nat Immunol. 2005; 6:981–988. [PubMed: 16127453]

Li XD, Chiu YH, Ismail AS, Behrendt CL, Wight-Carter M, Hooper LV, Chen ZJ. Mitochondrial antiviral signaling protein (MAVS) monitors commensal bacteria and induces an immune response that prevents experimental colitis. Proc Natl Acad Sci U S A. 2011; 108:17390–17395. [PubMed: 21960441]

Mariathasan S, Weiss DS, Newton K, McBride J, O'Rourke K, Roose-Girma M, Lee WP, Weinrauch Y, Monack DM, Dixit VM. Cryopyrin activates the inflammasome in response to toxins and ATP. Nature. 2006; 440:228–232. [PubMed: 16407890]

Meylan E, Curran J, Hofmann K, Moradpour D, Binder M, Bartenschlager R, Tschopp J. Cardif is an adaptor protein in the RIG-I antiviral pathway and is targeted by hepatitis C virus. Nature. 2005; 437:1167–1172. [PubMed: 16177806]

Nakahira K, Haspel JA, Rathinam VA, Lee SJ, Dolinay T, Lam HC, Englert JA, Rabinovitch M, Cernadas M, Kim HP, et al. Autophagy proteins regulate innate immune responses by inhibiting the release of mitochondrial DNA mediated by the NALP3 inflammasome. Nat Immunol. 2011; 12:222–230. [PubMed: 21151103]

Nakai K, Kanehisa M. A knowledge base for predicting protein localization sites in eukaryotic cells. Genomics. 1992; 14:897–911. [PubMed: 1478671]

Pichlmair A, Schulz O, Tan CP, Naslund TI, Liljestrom P, Weber F, Reis e Sousa C. RIG-I-mediated antiviral responses to single-stranded RNA bearing 5′-phosphates. Science. 2006; 314:997–1001. [PubMed: 17038589]

Rajan JV, Warren SE, Miao EA, Aderem A. Activation of the NLRP3 inflammasome by intracellular poly I:C. FEBS Lett. 2010; 584:4627–4632. [PubMed: 20971108]

Rock KL, Latz E, Ontiveros F, Kono H. The sterile inflammatory response. Annu Rev Immunol. 2010; 28:321–342. [PubMed: 20307211]

Seth RB, Sun L, Ea CK, Chen ZJ. Identification and characterization of MAVS, a mitochondrial antiviral signaling protein that activates NF-kappaB and IRF 3. Cell. 2005; 122:669–682. [PubMed: 16125763]

Shenoy AR, Wellington DA, Kumar P, Kassa H, Booth CJ, Cresswell P, Macmicking JD. GBP5 Promotes NLRP3 Inflammasome Assembly and Immunity in Mammals. Science. 2012

Shimada K, Crother TR, Karlin J, Dagvadorj J, Chiba N, Chen S, Ramanujan VK, Wolf AJ, Vergnes L, Ojcius DM, et al. Oxidized Mitochondrial DNA Activates the NLRP3 Inflammasome during Apoptosis. Immunity. 2012; 36:401–414. [PubMed: 22342844]

Shin KJ, Wall EA, Zavzavadjian JR, Santat LA, Liu J, Hwang JI, Rebres R, Roach T, Seaman W, Simon MI, et al. A single lentiviral vector platform for microRNA-based conditional RNA interference and coordinated transgene expression. Proc Natl Acad Sci U S A. 2006; 103:13759–13764. [PubMed: 16945906]

Stutz A, Golenbock DT, Latz E. Inflammasomes: too big to miss. J Clin Invest. 2009; 119:3502–3511. [PubMed: 19955661]

Wagner RN, Proell M, Kufer TA, Schwarzenbacher R. Evaluation of Nod-like receptor (NLR) effector domain interactions. PLoS One. 2009; 4:e4931. [PubMed: 19337385]

Wieckowski MR, Giorgi C, Lebiedzinska M, Duszynski J, Pinton P. Isolation of mitochondria-associated membranes and mitochondria from animal tissues and cells. Nature protocols. 2009; 4:1582–1590.

Zhou R, Tardivel A, Thorens B, Choi I, Tschopp J. Thioredoxin-interacting protein links oxidative stress to inflammasome activation. Nat Immunol. 2010; 11:136–140. [PubMed: 20023662]

Zhou R, Yazdi AS, Menu P, Tschopp J. A role for mitochondria in NLRP3 inflammasome activation. Nature. 2011; 469:221–225. [PubMed: 21124315]

Research Highlights

- Inactive NLRP3 is cytosolic and associates with mitochondria upon activation.
- The mitochondrial adapter MAVS mediates NLRP3 recruitment to mitochondria.
- The N-terminus of NLRP3 regulates MAVS association and mitochondrial recruitment.
- MAVS promotes NLRP3-mediated production of mature IL-1β.

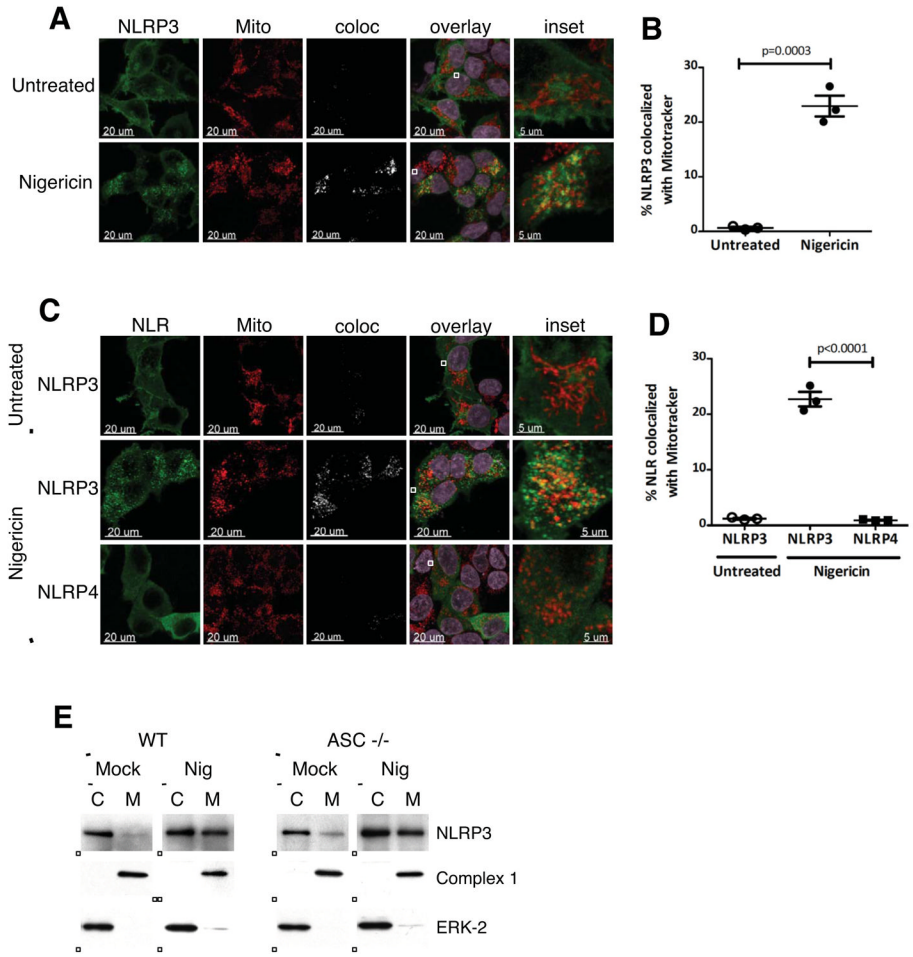

Figure 1. NLRP3 is cytosolic in the resting state and localizes to mitochondria upon activation

(A–B) Representative confocal immunofluorescence images (A) and quantification (B) of NLRP3 colocalized with Mitotracker in HEK-293T cells stably expressing NLRP3. Expression of NLRP3 was induced with doxycycline (DOX; 1 μg/ml), and cells were either untreated or treated with 15 μM nigericin for 45 min prior to imaging. **(C–D)** Representative immunofluorescence images (C) and quantification (D) of NLR colocalized with Mitotracker in HEK-293T cells expressing NLRP3 or NLRP4 under transient low expression conditions. Cells were transfected with 100 ng plasmid DNA for 8 h, and were either untreated or treated with 15 μM nigericin for 45 min prior to imaging. **(E)** Subcellular fractionation of WT and ASC KO BMDMs. BMDMs were either untreated (Mock) or primed with LPS (1 μg/ml for 4h) prior to stimulation with 7.5 μM nigericin for 30 min (Nig). Mitochondrial (M) and cytosolic (C) fractions were fractionated and analyzed for expression of NLRP3 by immunoblot. Purity of the fractions was assessed by blotting for Complex 1 (mitochondrial protein) and ERK-2 (cytosolic protein). Imaging data are representative of several images from 3 independent experiments. Data points on graphs represent independent fields (with 3–5 cells per field). Error bars are mean ± SEM. p-values from an unpaired t-test (two-tailed) are shown. Mito, Mitotracker; coloc, colocalization channel. See also Figure S1 and Table S1.

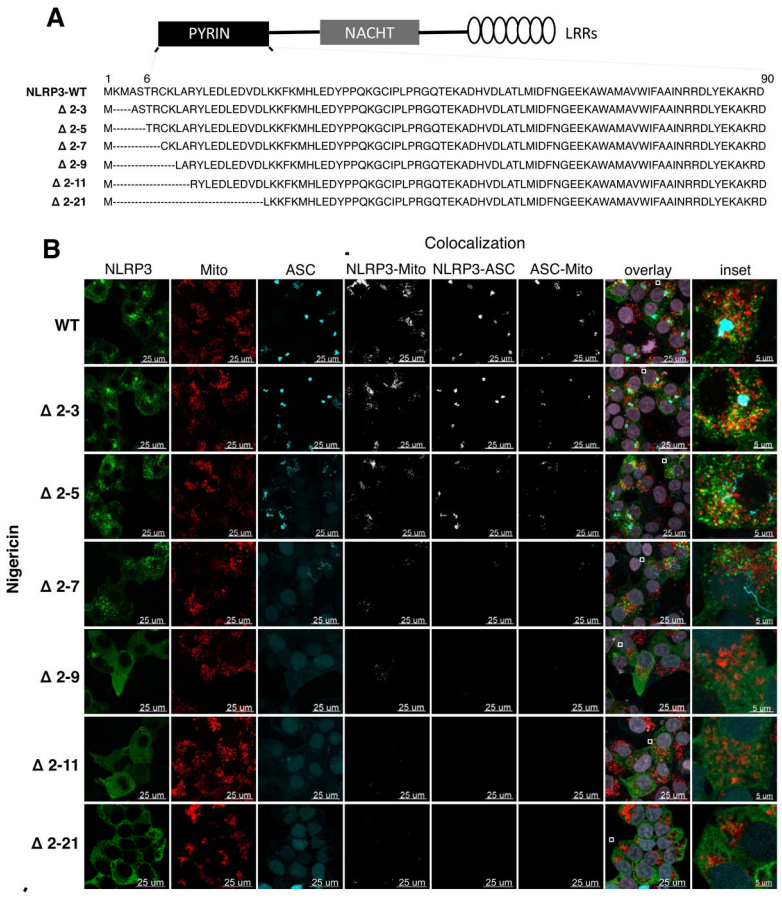

Figure 2. NLRP3 possesses an N—terminal sequence that controls mitochondrial association and ASC speckle formation

(A) Panel of N-terminal deletions of NLRP3. '----' indicates the deleted sequence. Structured region of the NLRP3 PYD encompasses residues 6–90. **(B)** Representative immunofluorescence images of HEK-293-ASC-YFP cells expressing WT and N-terminal deletions of NLRP3 under transient low expression conditions (100 ng plasmid DNA for 8h), and activated with 15 μM nigericin for 45 min prior to imaging. Representative images of unstimulated cells are shown in Figure S2. Imaging data are representative of several images from 4 independent experiments. Mito, Mitotracker. See also Figure S2.

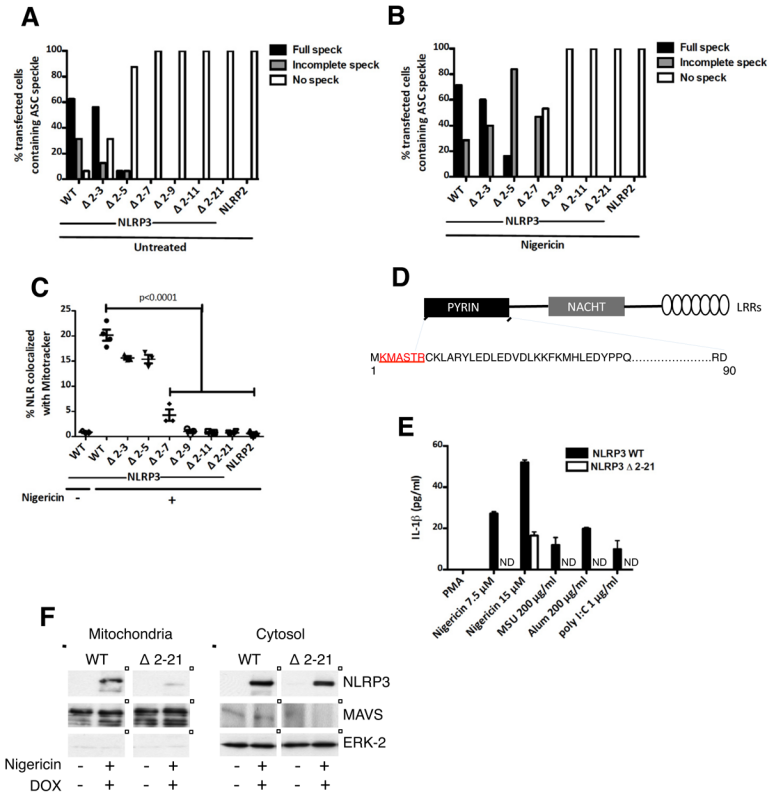

Figure 3. Effect of N—terminal deletions of NLRP3 on mitochondrial recruitment, ASC speckle formation, and IL-1β secretion

(A–B) Quantification of ASC speckle formation in HEK-293-ASC-YFP cells transiently transfected with low levels of WT or N-terminal deletions of NLRP3 (as in Figure S2 and Figure 2B), and either untreated (A) or treated with 15 μM nigericin (B) for 45 min prior to imaging. **(C)** Quantification of colocalization of WT and N-terminal deletion mutants of NLRP3 with Mitotracker in HEK-293-ASC-YFP cells transfected as above, and either untreated or treated with 15 μM nigericin for 45 min prior to imaging. **(D)** Minimum N-terminal sequence (2-7) necessary for NLRP3 mitochondrial association and ASC aggregation is indicated in red. **(E)** ELISA for IL-1β in supernatants of PMA-differentiated (non-LPS primed) THP-1 cells stably expressing NLRP3 WT or NLRP3 Δ2-21, and stimulated with the indicated NLRP3 activators. Expression of NLRP3 was induced for 12 h with DOX (1 μg/ml), prior to differentiation with 100 nM PMA for 3 h. **(F)** Subcellular fractionation of HEK-293T cells stably expressing either NLRP3 WT or NLRP3 Δ2-21. NLRP3 expression was induced with 1 μg/ml DOX for 6 h prior to stimulation with nigericin for 45 min. Data points in (A) and (B) represent the percentage of all transfected cells (pooled from multiple fields) containing a fully developed, incompletely developed, or no ASC speckle. At least 20 cells were evaluated for each construct. Data points in (C) represent independent fields (3–5 cells per field). Data are representative of 3 independent experiments. Error bars are mean ± SEM, and p-values from an unpaired t-test (two-tailed) are shown. ND; not detectable. See also Figure S3.

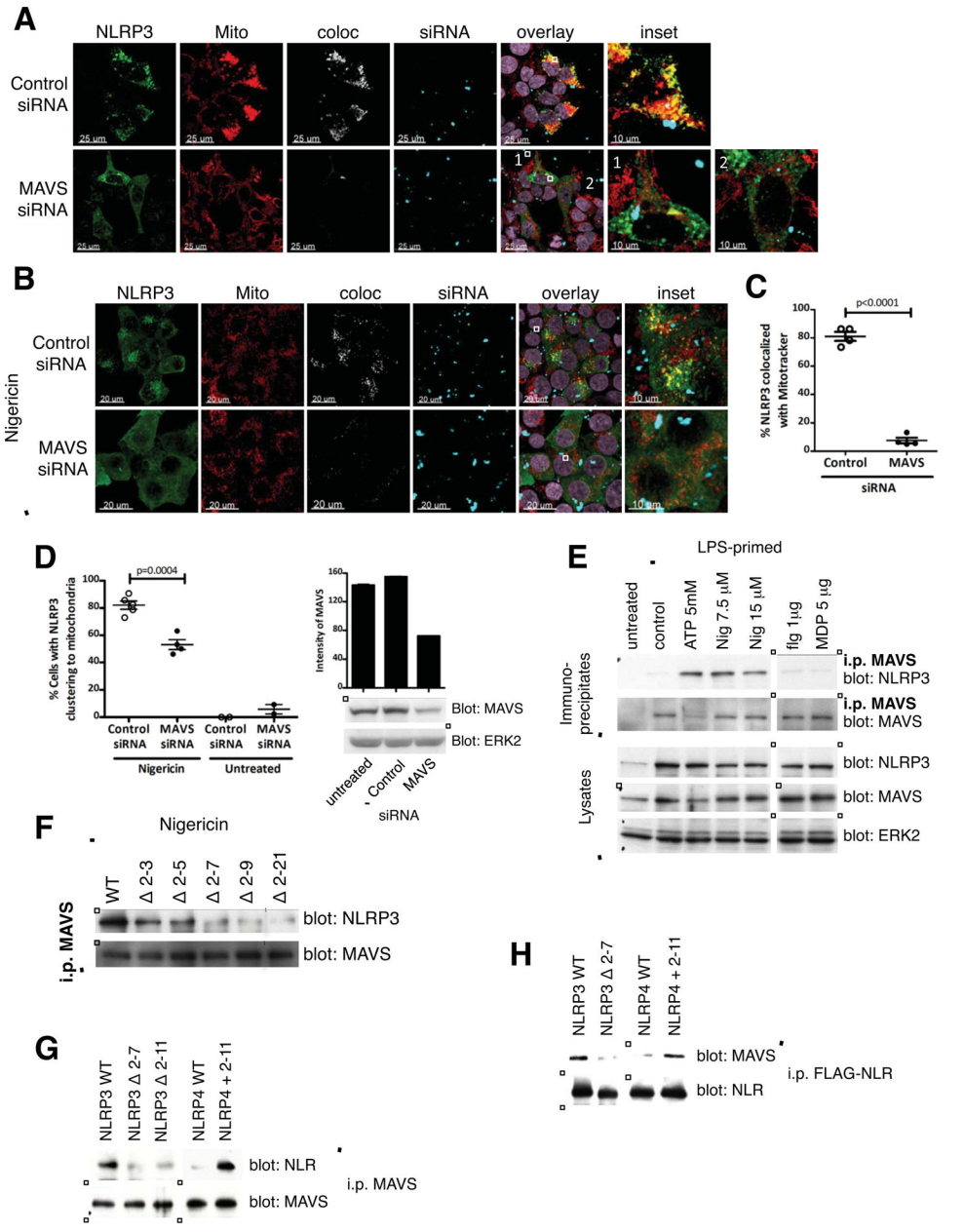

Figure 4. The mitochondrial adapter MAVS mediates NLRP3 mitochondrial localization

(A, C) Representative confocal immunofluorescence images (A) and quantification (C) of NLRP3 co-localized with Mitotracker in HEK-293T cells treated with control siRNA or MAVS siRNA prior to over-expression of NLRP3. siRNA transfected into cells appears as punctate spots shown in blue. **(B, D)** Representative immunofluorescence images (B) and quantification (D, left) of HEK-293T cells treated with control siRNA or MAVS siRNA prior to transient low expression of NLRP3 and stimulation with 15 μM nigericin for 45 min. Immunoblot and corresponding densitometric quantification for efficiency of MAVS knock-down are shown (D, right). **(E)** Immunoblot showing NLRP3 association with MAVS in BMDMs upon treatment with activators of NLRP3, but not activators of NLRC4 or NOD2/NLRP1. In some experiments MAVS expression in lysates decreases upon stimulation with ATP for unknown reasons. **(F)** Immunoblot showing progressive loss of

MAVS association by N-terminal deletion mutants of NLRP3 in HEK-293T cells. '|' indicates removal of an irrelevant lane(s) here and throughout. Cells were transiently transfected with low levels of FLAG tagged WT or N-terminal deletions of NLRP3, and treated with 15 μM nigericin for 45 min prior to lysate preparation. **(G)** Immunoblot showing MAVS association of NLRP4 with the added N-terminus of NLRP3 (NLRP4 + 2-11) in HEK-293T cells. Cells were transiently transfected with the indicated FLAG tagged constructs (1 μg DNA/10^6 cells for 20 h) prior to lysate preparation. **(H)** Immunoblot showing association of the indicated *in vitro* translated FLAG-tagged NLR proteins with purified MAVS. Immunoblots are representative of 2 independent experiments. Nig, nigericin; flg, flagellin; MDP, muramyldipeptide. Imaging data are representative of several images from 2 independent experiments. Data points on graphs in (C) and (D) represent individual fields with 3–5 cells per field (C) or 30–40 cells per field (D). Error bars are mean ± SEM, and p-values from an unpaired t-test (two-tailed) are shown. See also Figure S4 and Movies S1–S2.

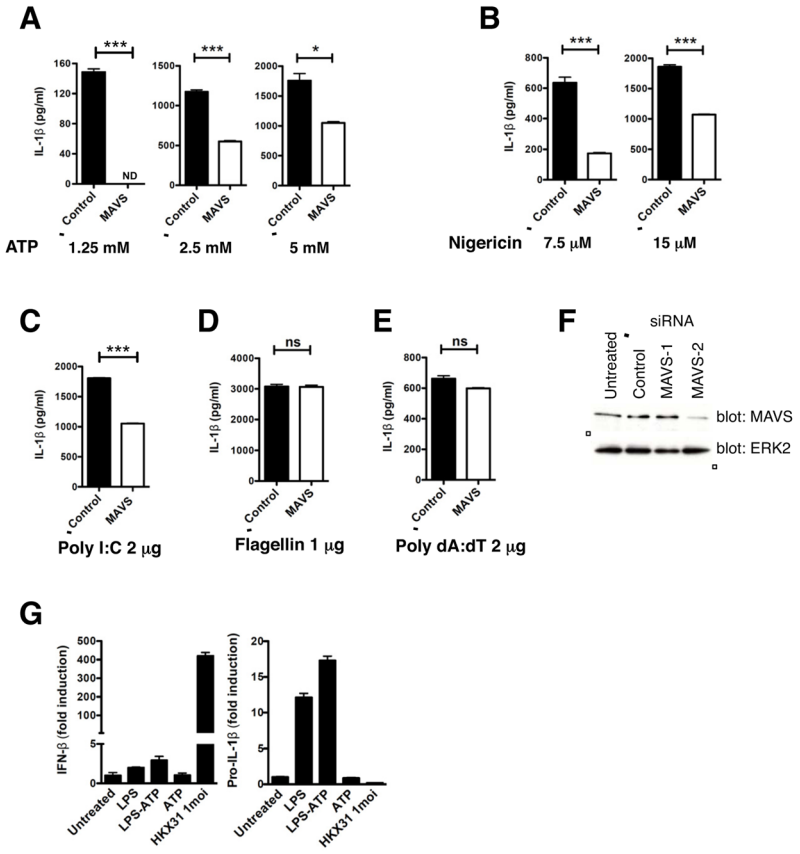

Figure 5. Silencing MAVS in BMDMs reduces IL-1β secretion in response to NLRP3 activators

(A–E) ELISA for IL-1β in supernatants of control or MAVS-silenced, LPS-primed BMDMs treated with the indicated concentrations of ATP and nigericin for 20 min (A, B), transfected poly I:C and poly dA:dT for 6 h (C, E), or transfected flagellin for 2 h (D). **(F)** Immunoblot for efficiency of MAVS knock-down in BMDMs. MAVS-2 siRNA specifically silenced MAVS and was used for assessing IL-1β secretion shown in A–E. **(G)** Quantitative RT-PCR for IFN-β (G, left) and pro-IL-1-β (G, right) expression in human monocytes treated with NLRP3 activator LPS-ATP or RIG-I activator Influenza A strain HKX31 (multiplicity of infection=1). mRNA expression was normalized to the housekeeping gene GAPDH. ELISA and RT-PCR data are representative of 2 independent experiments. Error bars are mean ± SEM, and p-values from an unpaired t-test (two-tailed) are shown. * $p<0.05$; ** $p<0.01$; *** $p<0.001$; ns, not significant; ND, not detectable.

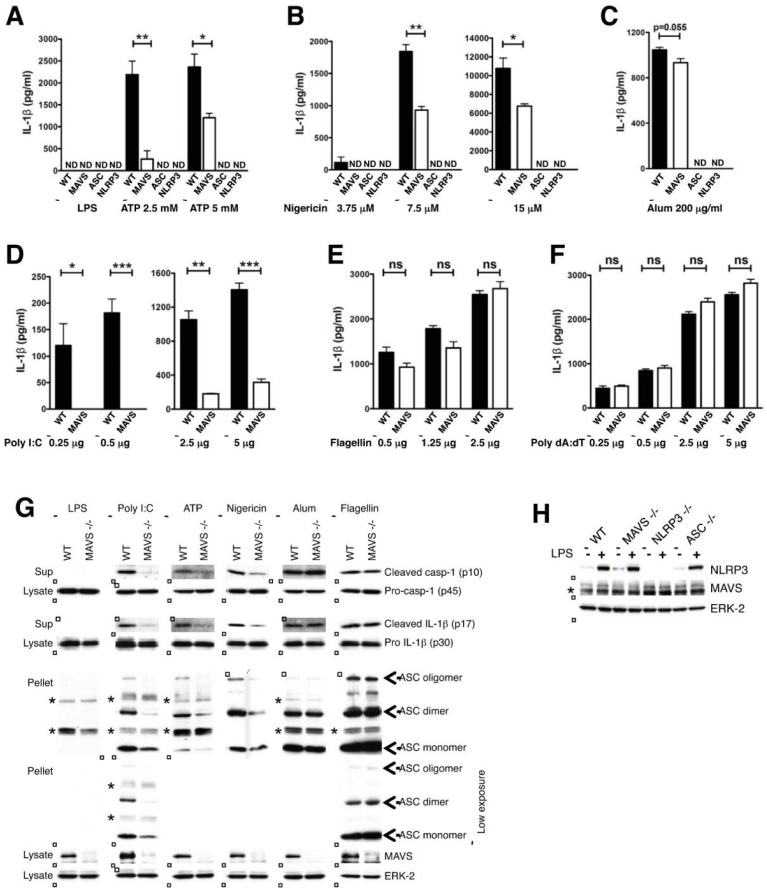

Figure 6. MAVS is required for optimal inflammasome activation by non-crystalline NLRP3 activators *in vitro.*

(A–F) ELISA showing IL-1β secretion from WT and MAVS −/− macrophages. LPS-primed BMDMs were treated with the indicated concentrations of ATP (A) or nigericin (B) for 20 min, alum crystals for 4 h (C), transfected poly I:C for 6 h (D), flagellin for 2 h (E) or poly dA:dT for 6 h (F). **(G)** Immunoblots showing processing of IL-1β and caspase-1 and ASC oligomerization in WT and MAVS −/− macrophages. LPS-primed BMDMs were treated with transfected poly I:C (2 μg/10^6 cells) for 6 h, ATP (2.5 mM) and nigericin (7.5 μM) for 20 min, alum crystals (200 μg/ml) for 6 h or transfected flagellin (1 μg/10^6 cells) for 2 h. Cell culture supernatants (Sup), cell lysates, and cross-linked pellets from whole cell lysates were analyzed by immunoblotting as indicated. Different doses of each NLRP3 activator were examined and representative blots at sub-saturating doses are shown. '*' indicates non-specific bands observed at higher exposures. **(H)** Immunoblot for NLRP3 following stimulation with LPS (1 μg/ml for 4 h). '*' indicates a non specific band. Data are representative of 2 independent experiments. Error bars are mean ± SEM, and p-values from an unpaired t-test (two-tailed) are shown. * $p<0.05$; ** $p<0.01$; *** $p<0.001$; ns, not significant; ND, not detectable. Casp-1, caspase-1. See also Figure S5.

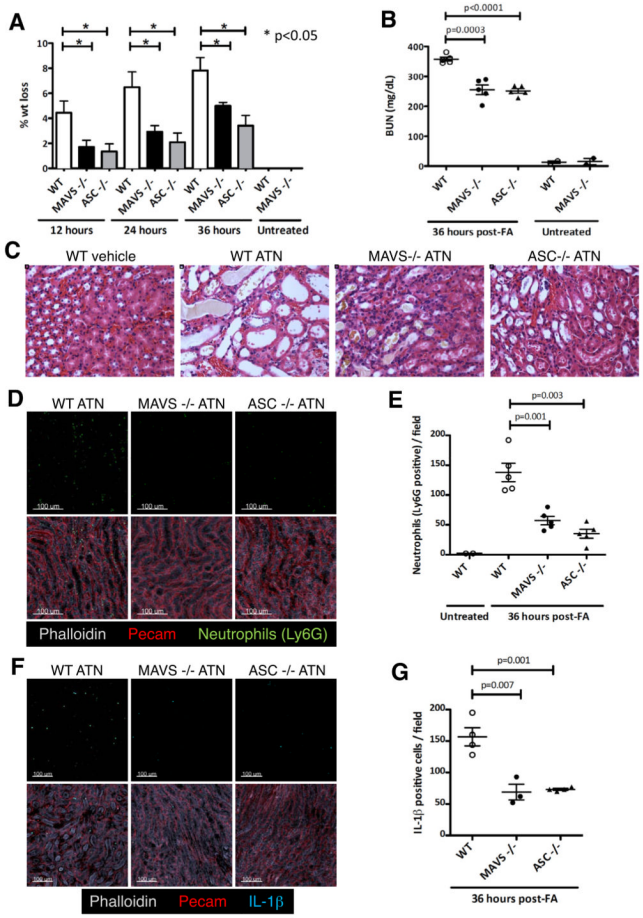

Figure 7. MAVS is essential for NLRP3 inflammasome function *in vivo* during acute tubular necrosis

(A) Percentage weight loss of WT, MAVS −/−, and ASC −/− mice injected intra-peritoneally with 250 mg folic acid/kg body weight (n=5 mice per group). **(B)** Measurement of BUN (blood urea nitrogen) in sera of mice with ATN. **(C)** Representative hematoxylin-eosin stained images from kidneys of WT, MAVS −/−, and ASC −/− mice at 36 h post-folic acid treatment. **(D–E)** Representative confocal immunofluorescence images (D) and quantification (E) of neutrophil influx at the cortico-medullary junction in kidneys of mice with ATN. **(F–G)** Representative confocal immunofluorescence images (F) and quantification (G) of IL-1β positive cells at the cortico-medullary junction. The sum of neutrophils (E) or IL-1β positive cells (G) counted in five independent high power fields (200x) at the cortico-medullary junction of each mouse kidney is shown. Data points in (B, E and G) represent individual mice. Error bars are mean ± SEM, and p-values from a two-tailed t-test are shown. Results are representative of 3 independent experiments. FA, folic acid. See also Figure S6.